17th International Conference on Microwave and High Frequency Heating
Valencia, Spain, September 9-12, 2019
AMPERE 2019
ISBN: 978-84-9048-719-8
DOI: http://dx.doi.org/10.4995/Ampere2019.2019.9940

# PLANE WAVE IRRADIATION OF A LAYERED SYSTEM: RESONANCE-BASED CONTROL OVER THERMAL RUNAWAY

A.A. Mohekar[1], B.S. Tilley[1,2], V.V. Yakovlev[2]

[1] *Department of Mechanical Engineering, Worcester Polytechnic Institute, Worcester, MA, USA*
[2] *Center for Industrial Mathematics and Statistics, Department of Mathematical Sciences, Worcester Polytechnic Institute, Worcester, MA, USA*
*aamohekar@wpi.edu, tilley@wpi.edu, vadim@wpi.edu*

**Keywords:** computational modeling, EM heating, thermal runaway

## Introduction

Traditional electromagnetic (EM) heating applications include thermal processing of food products, microwave assisted chemistry, and high temperature treatment of materials [1-3]. Currently, under development is a new technology of high-power EM heat exchangers (HX) intended for power beaming applications in wireless energy transfer [4, 5]. The key function of EM HX is to efficiently convert EM energy into heat (and, subsequently, into useful mechanical work). One of the challenges in front of the designers of such high-power devices is the nonlinear phenomenon of thermal runway.

The loss factor $\epsilon''$ is a key mechanism behind heat generation during EM heating. For typical ceramics, $\epsilon''$ increases exponentially with temperature, and that can potentially initiate thermal runaway putting the heating process out of control and damaging the material. Equilibrium EM heating can be represented by a parametric plot of the average steady-state temperature as function of the applied power that is known as a *power response curve*. In a layered structure, for the wavelengths of the incident wave that are much larger than the layer's thickness, the power response curve is an *S*-shaped bifurcation diagram [6, 7] (or *S*-curve) with two stable branches. Typically, temperatures are low at the lower branch of the *S*-curve and may be very high (up to 1,500-2,000 K) at the upper branch [8].

The recent analytical [8, 9] and numerical [10] models show that, for a triple (lossless-lossy-lossless) layered system, when thickness of the structure is comparable with the wavelength, an electric field resonance can be achieved in the lossy layer. This resonance causes the *S*-curve to acquire another (middle) stable branch and become a *double S*-curve. In this case, thermal runway triggered at lower power can stabilize at the middle branch (500-1000 K). That suggests that during thermal runaway temperature may be controlled by the electric field resonance and be limited to some reasonable (not damaging) values. Our goal is to determine if thermal runaway in an EM HX can be controlled with this mechanism in a layered layout [4, 5].

The models in [8-10] considered a triple layered geometry where symmetric irradiation from both sides of the layers was applied. In this paper, we analyze a more practical case, where the plane wave is applied to a grounded two-layer (lossless-lossy) structure. The grounded end of the lossy layer may cause total reflection of the EM waves. We show that the resonance producing a double *S*-curve can be achieved in the lossy layer by choosing its thickness such that a constructive interference between the incident and reflected waves is achieved. First, we analytically solve the EM-thermal coupled problem with a thin-domain approximation [8, 9] to get a power response curve. To validate the results, we simulate a numerical model in *COMSOL Multiphysics* and compare the power response curves produced by both approaches. Finally, a parametric study is carried out to identify factors affecting the shape of the double *S*-curve.

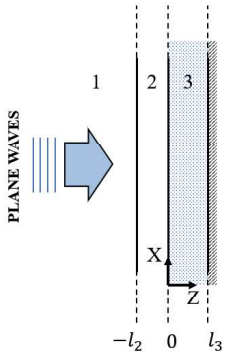


**Fig. 1.** Layout of the layered structure: region 1 is free space, region 2 is a lossless dielectric material, and region 3 is a lossy ceramic.

**Formulation of the Problem**

We consider a layered structure shown in Fig. 1. An incident plane wave travels along the positive Z-direction, is polarized along the Y-direction, and is uniform in the X-direction. Maxwell's equations for the considered problem are reduced to the one-dimensional Helmholtz equation

$$\frac{\partial^2 E_j}{\partial z^2} + k_0^2 \mu_{r_j}\left[\epsilon'_{r_j} - i\frac{\sigma_{e_j}(T_j)}{\omega\epsilon_0}\right]E_j = 0, \qquad j = 1,2,3 \tag{1}$$

where subscript $j$ represents the region of the solution, $E = \bar{E}/E_0$, $\bar{E}$ is the dimensional form of the electric field, $E_0$ is the strength of the plane wave, $z = \bar{z}/L_z$, $\bar{z}$ is the dimensional length along Z, $L_z$ is the length scale in Z, $k_0 = 2\pi L_z/\lambda_0$ is the non-dimensional wave number, $\mu_r$ is the relative permeability, $\epsilon'_r$ is the relative permittivity of the medium, $\sigma_e$ is the effective electrical conductivity, $T$ is temperature, $\omega$ is the angular frequency, and $\epsilon_0$ is permittivity of free space. Since region 2 is a lossless dielectric, $\sigma_{e_2} = 0$.

Since $\sigma_e$ is temperature-dependent, we solve the thermal energy equations to evaluate $T$. We introduce non-dimensional form $T = (\bar{T} - T_A)/T_A$, where $\bar{T}$ is the dimensional temperature and $T_A$ is the ambient temperature, choose the conduction time scale as $L_x^2/\alpha_3$, where $\alpha_3$ is the thermal diffusivity of region 3 and $L_x$ is the length scale along X-direction, and assume that the electric field is uniform in the X-direction, which means that the heat flux along X is zero ($\frac{\partial T}{\partial x} = 0$) and $T$ is only function of $t$ and $z$. With these assumptions, the 1D time-dependent non-dimensional energy equations become

$$\eta^2 \frac{\partial T_2}{\partial t} = \alpha \frac{\partial^2 T_2}{\partial z^2}, \tag{2}$$

$$\eta^2 \frac{\partial T_3}{\partial t} = \frac{\partial^2 T_3}{\partial z^2} + \eta^2 P \sigma_3(T_3)|E_3(T_3)|^2, \tag{3}$$

where $\eta = L_z/L_x$ is the aspect ratio of the geometry, $T_2$ and $T_3$ are non-dimensional temperatures in regions 2 and 3, respectively, $\alpha = \alpha_2/\alpha_3$ is the ratio of thermal diffusivities of regions 2 and 3, respectively, $P = \frac{L_x^2 \sigma_0 E_0^2}{2k_3 T_A}$ is non-dimensional power, $k_3$ is thermal conductivity of region 3, $\sigma_3 = \sigma_{e_3}(T_3)/\sigma_0$ is non-dimensional electrical conductivity, and $\sigma_0 = \omega\epsilon_0$. The length scale in the Z-direction, i.e., thickness of the lossy layer, is chosen to be $l_3$. We solve the coupled system (1)-(3) with the EM boundary conditions

$$\frac{\partial E_2}{\partial z} + ik_0 E_2 = 2ik_0, \qquad \text{at } z = -\frac{l_2}{l_3} = -l, \tag{4}$$

$$E_2 = E_3, \frac{\partial E_2}{\partial z} = \frac{\partial E_3}{\partial z}, \qquad \text{at } z = 0, \tag{5}$$

$$E_3 = 0, \qquad \text{at } z = 1, \tag{6}$$

and the thermal boundary conditions

$$k\frac{\partial T_2}{\partial z} = \eta^2 Bi\, T_2, \qquad \text{at } z = -l \tag{7}$$

$$k\frac{\partial T_2}{\partial z} = \frac{\partial T_3}{\partial z}, T_2 = T_3, \qquad \text{at } z = 0, \tag{8}$$

$$\frac{\partial T_3}{\partial z} = 0, \qquad \text{at } z = 1, \tag{9}$$

where $\eta^2 Bi = hl_3/k_3$ is the scaled Bio number, $h$ is the heat transfer coefficient at $z = -l$, and $k = k_2/k_3$ is the ratio of thermal conductivities of regions 2 and 3, respectively.
Boundary conditions (5) describe continuity of the electric field and its derivative at the interfaces between the regions, (6) suggests that the layered structure is attached to the ground/metal plate at $z = 1$. We assume that thermal lossless to the surrounding are scaled with $\eta^2$; since $\eta$ is assumed to be small, thermal losses are also small. Eq. (7) describes the thermal losses to the surrounding by Newton's law of cooling, (8) states that the interfaces between the regions are in perfect thermal contact, i.e., heat flux and temperature are continuous, and (9) is adiabatic boundary condition at the metal plate.
We first solve the coupled system (1)-(3) analytically using a thin domain approximation ($\eta \ll 1$) and compute the power response curve. Then we solve the system in *COMSOL Multiphysics* and compare the power response curves produced by both the models.

**Assumptions**

Since the main objective of this paper is demonstration of a principle possibility of the control over thermal runaway in the structure in Fig. 1, we do not consider here practical materials leaving that for future consideration. Thermal properties as well as $\epsilon_r$ are assumed to be temperature independent, and all the materials are non-magnetic ($\mu_r$ = 1). Since another objective of this study is to find desirable permittivity of region 2, we consider a wide range of values for $\varepsilon_{r2}$. As it is shown below, the power response curves are independent of thermal parameters of regions 2 and 3, so we choose specific heat $C_p$, density $\rho$, and thermal conductivity $k$ of region 2 to be the same as those of zirconia. The material properties used in computations are listed in Table 1. For computation of power response curves, we take $\eta$ = 0.1. The relation between $\sigma_3$ and $T$ is determined by curve fitting using the least squares.

**Thin Domain Approximation**

The 1D Helmholtz equation (1) can be solved exactly in terms of $T$ and the general solution has the form

$$E_j(z) = a_j e^{i\xi_j z} + b_j e^{-i\xi_j z},$$

where $\xi_j = \sqrt{k_0^2\left[\epsilon'_{r\,j} - i\frac{\sigma_{e_j}(T_j)}{\omega\epsilon_0}\right]}$, and the coefficients $a_j$ and $b_j$ depend on the boundary conditions (4)-(6). Under the thin-domain approximation $\eta \ll 1$, we can expand temperatures in the form of asymptotic series

$$T_j = T_j^{(0)} + \eta T_j^{(1)} + \eta^2 T_j^{(2)} + o(\eta^3).$$

**Table 1**. Properties of the Materials in Region 3 (Zirconia, [11]) and Region 2.

| Region | $\epsilon_r{}'$ | $\sigma_e(\bar{T})$ [S/m] | $\rho$ [Kg/m$^3$] | $C_p$[J/kgK] | $k$[W/mK] |
|---|---|---|---|---|---|
| 2 | 6.69-133.8 | 0 | 2848 | 217 | 0.2 |
| 3 | 6.69 | $0.00046e^{2.285\left[\frac{(T-T_A)}{T_A}\right]}$ | 2848 | 217 | 0.2 |

Substituting $T_j$ in (4)-(5), we get zero order terms and first order terms as

$$\frac{\partial^2 T_j^{(0)}}{\partial z^2} = 0, \frac{\partial^2 T_j^{(1)}}{\partial z^2} = 0.$$

Applying boundary conditions (7)-(9), we see that both zero and first order solutions are independent on $z$, and the leading order solution can be written as

$$T_j^{(0)} = T^{(0)}(t).$$

Second order correction term results in the system of equations

$$\alpha \frac{\partial^2 T^{(2)}}{\partial z^2} = \frac{\partial T^{(0)}}{\partial t}, \tag{10}$$

$$\frac{\partial^2 T^{(3)}}{\partial z^2} = \frac{\partial T^{(0)}}{\partial t} - P\sigma_3\left(T^{(0)}\right)\left|E_3\left(T^{(0)}\right)\right|^2. \tag{11}$$

Integrating (10) over $(-l, 0)$ and (11) over $(0, 1)$, and applying boundary conditions (7)-(9), we get an ordinary differential equation governing average temperature in the form

$$\left(\frac{kl}{\alpha} + 1\right)\frac{\partial T}{\partial t} = P\sigma_3(T)\left||E_3|\right|_2^2 - Bi\, T, \tag{12}$$

where $\left||E_3|\right|_2^2 = \int_0^1 |E_3(z)|^2 dz$, $|E_3(z)|^2 = E_3(z)E_3^*(z)$, and $E_3^*$ is the complex conjugate of $E_3$. At steady state, solution of (12) can be written down as

$$P = \frac{Bi\, T}{\sigma_3(T)\left||E_3|\right|_2^2}, \quad \text{or } P_{in} = \frac{h(\bar{T} - T_A)}{\gamma l_3 \sigma_{e_3}(\bar{T})\left||E_3|\right|_2^2}, \tag{13}$$

where $T$ and $\bar{T}$ are now average non-dimensional and dimensional steady-state temperatures, respectively, $\sigma_{e_3}$ is the dimensional effective loss factor of region 3, and $E_3$ is the non-dimensional electric field in region 3. The second formula in (13) for the dimensional power density of the incident wave $P_{in} = E_0^2/2\gamma$ (here $\gamma$ is the characteristic impedance of free space) is obtained by substitution of the dimensional quantities in the first formula. So (13) defines the power response curve as a parametric plot of $P$ (or $P_{in}$) and $T$ (or $\bar{T}$). We see that the power responses are indeed independent of thermal properties of regions 2 and 3.

***COMSOL Multiphysics* Model**

We now solve the coupled system (1)-(3) along with the boundary conditions (4)-(9) in *COMSOL Multiphysics*. We use quadratic Lagrange elements to spatially discretize the geometry and determine maximum size of the element according to the meshing criteria discussed in [10]. Also, due to a high degree of nonlinearity, we use *COMSOL*'s adaptive time-dependent solver and steady-state is assumed to be reached when an absolute difference between average temperatures at previous and current time step falls below $10^{-4}$. This solver discretizes temporal gradients using second order backward difference method. To get a

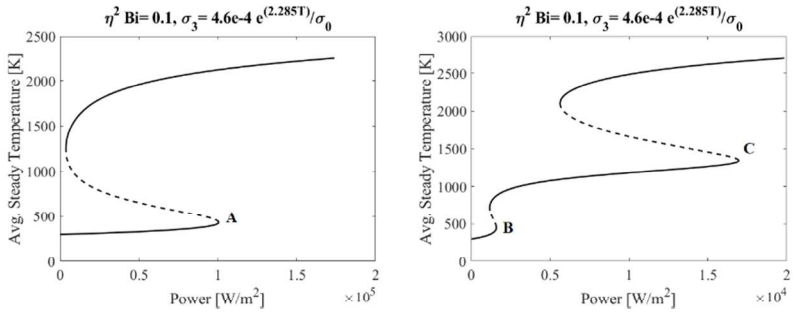


(a) (b)

**Fig. 2.** Power response curves without (a) and with (b) an electric field resonance in region 3 for $\varepsilon_{r2} = 71$; stable (solid curves) and unstable solutions (dashed curves).

power response curve in the *COMSOL* model, simulation is performed for different values of $P_{in}$, and the average steady-state temperature is plotted as a function of $P_{in}$.

## Computational Results

### *A. Effect of Electric Field Resonance*

Gaone et al in [8, 9] thoroughly studied the effect of the electric field resonance on the power response curve of a layered structure. For a triple layer (lossless-lossy-lossless), a power response curve becomes a double *S*-curve if electric field resonance is achieved in the lossy layer. The resonance criteria considered in [8-10] are given for any odd multiple $n_1$, $n_2$ as

$$l_2 = \frac{n_1\lambda_2}{4} \text{ and } l_3 = \frac{n_2\lambda_3}{2}, \tag{14}$$

where $\lambda_2$ and $\lambda_3$ are the wavelengths of EM wave in region 2 and 3, respectively.
For the geometry considered in this paper, we follow the criteria (14) and choose $n_1 = 1$ and $n_2 = 3$. The ground/metal plate boundary acts as a perfect reflector of the EM waves in region 3. The total reflection causes constructive interference between incident and reflected waves, and resonance builds up in the lossy layer. From Fig. 2, we see that as we achieve electric field resonance in the lossy layer, *S*-curve transitions into a double *S*-curve.
A branch of a power response curve is stable (or unstable) if it has a positive (or negative) slope [7]. It can be seen from Fig. 2(a) that, when the incident power of the EM wave is higher than critical power at point A, thermal runaway is triggered there, but stabilized at the upper stable branch (~2000 K). However, from Fig. 2(b), we see that the double *S*-curve has a new stable (middle) branch between lower and upper branch. When incident power is above critical power at B but less than power at C, thermal runway may stabilize at the middle branch (~ 1000 K). We also notice that because of the electric field resonance, more EM energy is trapped inside the lossy layer as compared to a non-resonant case. Therefore, critical power levels (powers corresponding to points B and C) are significantly lowered.

### *B. Comparison with COMSOL Model*

We now compare the power response curves generated by the analytical and *COMSOL* models. From Fig. 3, we see that, for $h$ = 2.54 W/(m$^2$K), the curves do not match well with each other. The disagreement is due to the differences in corresponding assumptions. The analytical model approximates the solution for a very thin and long channel assuming uniform temperatures in the Z-direction. On the other hand, *COMSOL* model considers spatial variation of temperature in Z. The effect of spatially varying temperature on the power response curve was discussed in [10]. We now maintain $h$ = 0.64 W/(m$^2$K), and

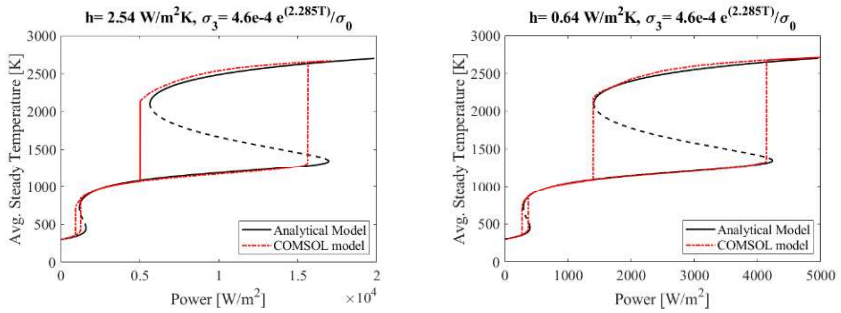


**Fig. 3.** Power response curves obtained by the analytical and *COMSOL* models for $\varepsilon_{r2} = 71$, $\eta^2 Bi = 0.1$ (a), and $\eta^2 Bi = 0.025$ (b).

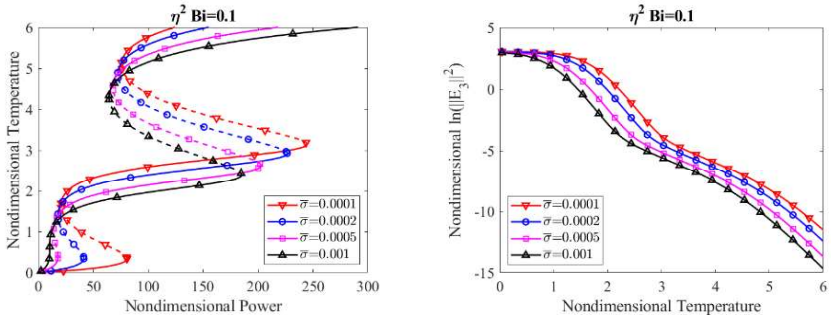


**Fig. 4.** Power response curves (a), and $\ln\left|\left|E_3\right|\right|^2$ (b) as functions of temperature for $\beta = 3$, $\varepsilon_{r2} = 71$ and varying factor $\bar{\sigma}$.

further limit thermal lossless to the surrounding making spatial variation of temperatures more uniform. We expect that as $h \to 0$, the response curves given by both models get closer. From Fig. 3(b), we observe that the power response curves are in satisfactory agreement.

### *C. Parametric Study*

In this section we discuss how $\sigma_3$, $\eta^2 Bi$, and $\epsilon_{r_2}$ affect the shape of the power response curve. Throughout this parametric study, thermal properties are the same as in Table 1. For many typical ceramics, the loss factor increases exponentially with temperature, therefore, we assumed $\sigma_3$ to have a form of $\bar{\sigma} e^{\beta T}$ [8-10].

First, we hold $\beta$ constant and vary $\bar{\sigma}$. From Fig. 4(a) it is seen that when $\bar{\sigma}$ is increased, the region of unstable solution diminishes, and for $\bar{\sigma} = 0.001$ the only stable solution is found in the low power region. To understand why an unstable solution disappears in low power region with increasing $\bar{\sigma}$, we take natural logarithm of both sides of (13) and take its derivative with respect to temperature

$$\frac{d}{dT}[\ln(P)] = \frac{1}{T} - \beta - \frac{d}{dT}\left[\ln\left|\left|E_3\right|\right|^2\right].$$

A branch is stable (or unstable) if

$$\frac{1}{T} > (\text{or} <)\ \beta + \frac{d}{dT}\left[\ln\left||E_3|\right|^2\right]. \quad (15)$$

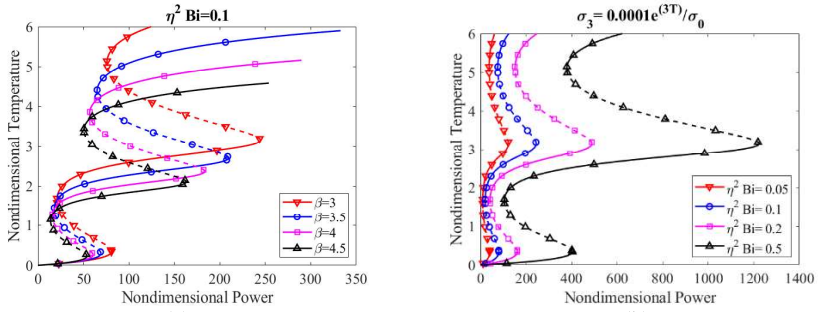


(a) (b)

**Fig. 5** Power response curves for $\epsilon_{r_2} = 71$ and varying $\beta$ (a) and $\eta^2 Bi$ (b).

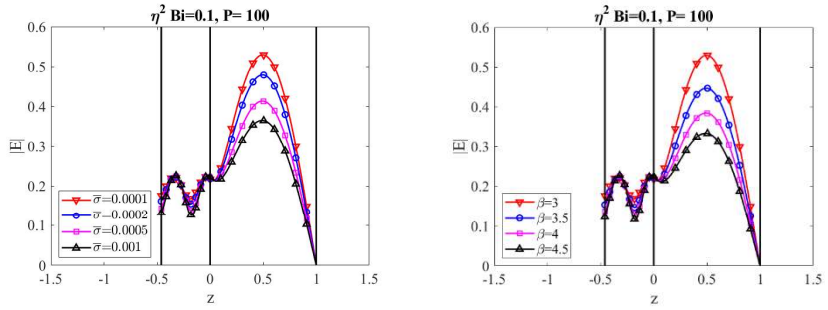


(a) (b)

**Fig. 6.** Magnitude of the non-dimensional electric field as a function of $z$ for $\beta = 3$ and varying $\bar{\sigma}$ (a) and for $\epsilon_{r_2} = 71$ and varying $\beta$ (b).

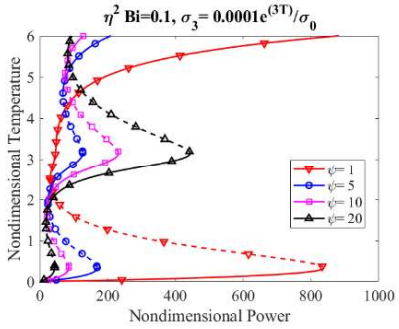


**Fig. 7.** Power response curves for varying $\psi = \epsilon_{r_2}/\epsilon_{r_3}$.

From Fig. 4(b), we notice that in the lower unstable temperature range, $-\frac{d}{dT}\left[\ln\left||E_3|\right|^2\right]$ is larger when $\bar{\sigma} = 0.001$ compared to other cases. This makes combined contribution of $\beta$

and $\frac{d}{dT}\left[\ln\left||E_3|\right|^2\right]$ in (15) smaller than $1/T$; as a result, only a stable solution exits in the lower temperature region. From (15), we observe that the range of stable temperatures may increase if $\beta$ is increased. We confirm this in Fig. 5(a), where the length of the stable branches increases with increasing $\beta$. It can be also seen that with increasing $\bar{\sigma}$ or $\beta$, the EM losses also increase, which causes $|E_3|$ to decrease, as seen in Fig. 6. Since less EM energy is available for the source of thermal energy, temperatures of the middle and top branches keep dropping down, as seen in Fig. 4(a) and Fig. 5(a).

Describing the effects of thermal losses to the surrounding, we see from Fig. 5(b) that as $\eta^2 Bi$ goes up, the length of the middle branch also increases. This behavior may be expected since we see from (13) that $P$ is proportional to $Bi$. We define the ratio of permittivities of regions 2 and 3 as $\psi = \varepsilon_{r2}/\varepsilon_{r3}$. Keeping $\varepsilon_{r3}$ constant, we change $\varepsilon_{r2}$ by varying $\psi$. When $\varepsilon_{r2}$ changes, the thickness of region 2 also changes by (14). From Fig. 7, we see that when $\psi = 1$, the electric field resonance breaks, and an *S*-curve emerges. We also observe that the length of the middle branch increases with $\psi$. This is expected because the strength of the resonance in region 3 is greatest when $\varepsilon_{r2}$ is large and $\varepsilon_{r3}$ is small [8, 9]. Thus for a double *S*-curve to have a shape such that thermal runaway could be stabilized at the middle branch, having higher permittivity of the outer layer is preferable.

## Conclusions

We have described two (1D analytical and numerical) models of a grounded two-layer system undergoing EM heating by plane waves. It has been demonstrated that the resonance producing a double *S*-curve can be achieved with a one-sided irradiation. Because of the electric field resonance, thermal runaway starts at lower power levels, but may stabilize at the middle branch of the double *S*-curve. With the thin-domain asymptotic approximation, the system of equations is reduced to a time-dependent ordinary equation. Its steady-state solution gives the power response curve. A numerical model has been built in *COMSOL Multiphysics*. Double *S*-curves generated by both the models are found to be in satisfactory agreement. We have shown that temperatures of the middle and upper branches may be decreased by increasing the electrical conductivity of the lossy layer as less EM energy is available for heat generation. It has been demonstrated that the length of the middle branch increases with thermal losses to the surrounding. Thus the resonance-based control is, in principle, possible for the considered structure (with the ground/metal surface on the back of region 3), but it depends on the relation between dielectric constants of regions 2 and 3.

## Acknowledgement

The authors are grateful for the support from the US Air Force Office of Scientific Research, Award FA9550-18-1-0528.

## References

[1] Willert-Porada, M., Ed., *Advanced in Microwave and Radio Frequency Processing*, Springer, 2006.
[2] Tao, J., Ed., *Microwave and RF Power Applications*, Cépaduès Éditions, 2011.
[3] Leadbeater, N.E., Ed., *Microwave Heating as a Tool for Sustainable Chemistry*, CRC Press, 2010.
[4] Jawdat, B., et al, *Proc. 2017 IEEE Wireless Power Transfer Conf.*, 978-1-5090-4595-3/17.
[5] Kumi, P., et al, In: *Scientific Computing in Electrical Engineering*, G. Nicosia, V. Romano, Eds, Springer, 2019 (in press).
[6] Kriegsmann, G.A., *J. of Applied Physics*, 1992, **71**, 1960-1966.

[7] Pelesko, J.A., G.A. Kriegsmann, *J. of Eng. Math*., 1997, **32**, 1–18.
[8] Gaone, J.M., et al, *J. of Eng. Math*., 2019, **114**, 65–86.
[9] Gaone, J.M., et al, *IEEE MTT-S Intern Microwave Symp. Dig. (Honolulu, HI, June 2017)*, 978-1-5090-6360-4.
[10] Mohekar, A.A., et al, *IEEE MTT-S Intern. Micro. Symp. Dig. (Philadelphia, PA, June 2018)*, pp. 1389–1392.
[11] V.V. Yakovlev, et al, In: *Microwave and RF Power Applications*, J. Tao, Ed., Cépaduès Éditions, 2011, pp. 303-306.